Sustainable Cities and Society 61 (2020) 102286

Contents lists available at ScienceDirect

Sustainable Cities and Society

journal homepage: www.elsevier.com/locate/scs

# Exploring the relationships between urban spatial form factors and land surface temperature in mountainous area: A case study in Chongqing city, China

Jianming Guo[a], Guifeng Han[a,*], Yusi Xie[a], Zhi Cai[b], Yifan Zhao[a]

[a] School of Architecture and Urban Planning, Key Laboratory of New Technology for Construction of Cities in Mountain Area of Education Ministry, Chongqing University, No.83 Shabei Street, Shapingba District, Chongqing City, 400045, China
[b] School of Architecture, Tsinghua University, Haidian District, Beijing, 100084, China

ARTICLE INFO

*Keywords:*
Urban spatial form
Land surface temperature
Urban heat island
Spatial regression
Mountainous city

ABSTRACT

In recent years, frequent heat waves have severely reduced the quality of human settlements in big cities. To reveal the influence of urban spatial form on land surface temperature (LST) in mountainous cities, Chongqing city in China was selected as a case study. The quantitative relationships between five urban spatial form factors and LST are analyzed, such as sky view factor (SVF), urban surface roughness (USR), road surface area density (RSD), building density (BD) and floor area ratio (FAR). The results showed that the spatial scale influence their correlations. Most urban spatial form factors have a significant positive relationship with LST, besides FAR. The various regression results have also shown that spatial regression models (Spatial lag model, Spatial error model and General spatial model) are working better than OLS model, due to the reason that some of the urban spatial form factors have spatial spillover and spatial heterogeneity effect. Besides the spatial effect, the unique topography of mountainous city also has an impact on LST, such as the slope, aspect and underlying surface. Therefore, the planners should consider those differences in mountainous cities, and using different methods to mitigate UHI and making the city cope with climate change.

## 1. Introduction

With the rapid development of urbanization, billions of people surged to urban areas in the past few decades. Which leads to the natural covers (e.g., green spaces and water bodies) covert to built-up impervious covers (e.g., building and road), and more anthropogenic heat release concentrated in urban areas (Debbage & Shepherd, 2015). As a result, urban has a higher temperature than their surrounding rural areas, this phenomenon is known as urban heat island (UHI) effect (Feyisa, Dons, & Meilby, 2014; Li, Zhang, & Kainz, 2012; Li, Zhou, Ouyang, Xu, & Zheng, 2012; Skoulika, Santamouris, Kolokotsa, & Boemi, 2014; Voogt & Oke, 2003). The significant UHI will threaten the sustainable development of the city and increase its ecological environmental problems (Li & Norford, 2016). Moreover, UHI combined with climate change making the extreme heatwaves are more common in summer, which will put lots of people in danger, especially the elderly (Chang, Li, & Chang, 2007), and increase their morbidity and mortality (Zhang, Zheng, & Chen, 2019). Therefore, there is an urgent need to study UHI and find some ways to mitigate it.

There are several parameters to reflect UHI, such as air temperature and land surface temperature. Air temperature from situ measurement and weather stations are the common index in the early studies (Howard, 1833; Matthews, 1937). With the development of remote sensing technology, the LST retrieved from remote sensing images are widely used by scholars. Based on LST, they try to reveal the spatial-temporal temperature patterns and its differences between urban and rural areas (Coseo & Larsen, 2014; Chen, Zhao, Li, & Yin, 2006; Connors, Galletti, & Chow, 2013; Imhoff, Zhang, Wolfe, & Bounoua, 2010; Li et al., 2011; Lo, Quattrochi, & Luvall, 1997; Shen, Huang, Zhang, Wu, & Zeng, 2016; Streutker, 2003; Yuan & Bauer, 2007), and also found LST in urban areas are higher than its surrounding rural areas, that is surface urban heat island (SUHI).

The SUHI is a consequence of absorbed solar radiation and anthropogenic heat release with a synthesized influence of many factors, such as natural factors (e.g., climate zone, solar radiation and wind speed) (Ren, Deng, Zuo, Song, & Li, 2016), physical construction factors

* Corresponding author.
*E-mail addresses:* guojianming2010@foxmail.com (J. Guo), hangf@cqu.edu.cn (G. Han), emily5225@126.com (Y. Xie), czhi911@foxmail.com (Z. Cai), sitelatuosi@163.com (Y. Zhao).

https://doi.org/10.1016/j.scs.2020.102286
Received 3 June 2019; Received in revised form 15 May 2020; Accepted 22 May 2020
Available online 12 June 2020
2210-6707/ © 2020 Elsevier Ltd. All rights reserved.

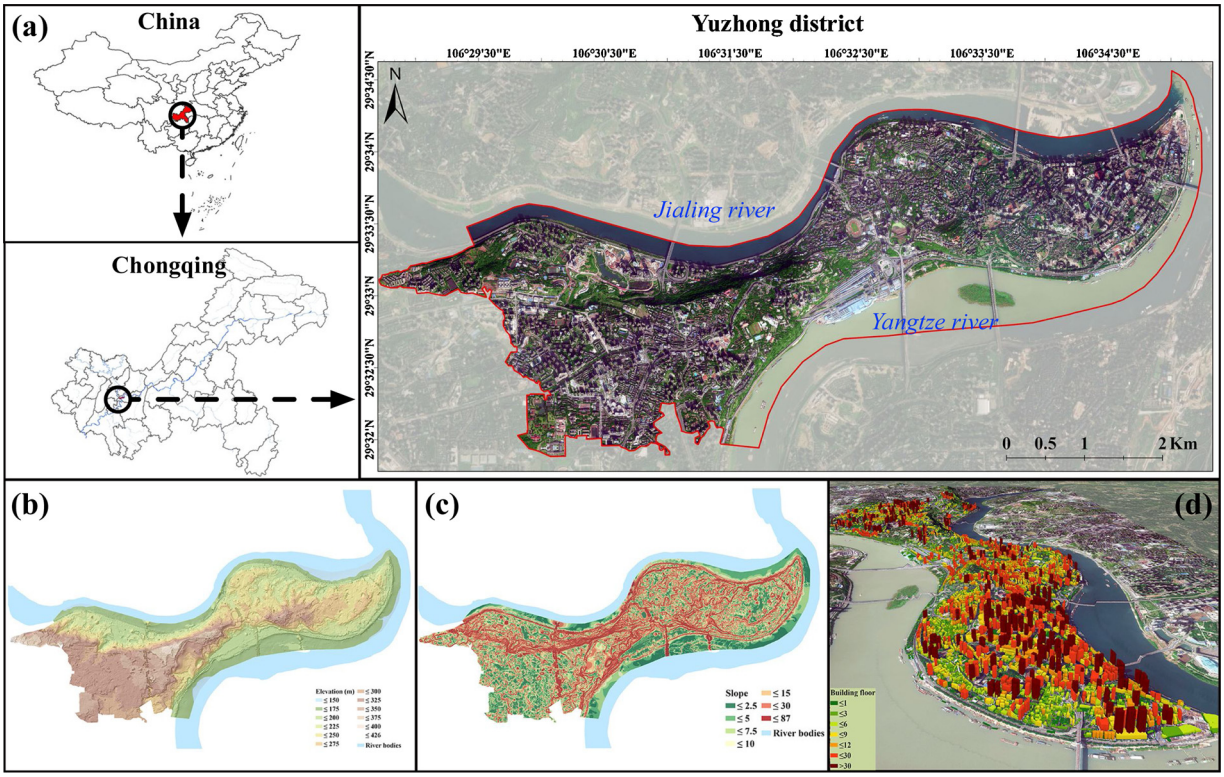



**Fig. 1.** The location (a), elevation (b), slope (c) and bird view (d) of study area.

(urban spatial form) (Middel, Hab, Brazel, Martin, & Guhathakurta, 2014; Schwarz & Manceur, 2015; Taleghani, Kleerekoper, Tenpierik, & Den Dobbelsteen, 2015) and social-economic factors (e.g., population density, economy and racial characteristics) (Cai, Tang, Chen, & Han, 2019; Huang, Zhou, & Cadenasso, 2010; Huang, Zhou, & Cadenasso, 2011; Kinney, O'Neill, Bell, & Schwartz, 2008; Mitchell & Chakraborty, 2014). Of these factors, urban spatial form exerts a more significant influence than the other factors in a particular city (Guo, Zhou, Wu, Xiao, & Chen, 2016; Hebbert, 2014; Li et al., 2016; Middel, Lukasczyk, & Maciejewski, 2017; Oke, 1979). Urban spatial form refers to a complex and dynamic form of spatial expression, which covers many aspects such as land cover, landscape diverse types, building layout and topography. And it profoundly influences human activities and plays an important role in the formation and transformation of cities (Conzen, 2001; Fang, Wang, & Li, 2015; Kropf, 2009; Lynch, 1981; Tsai, 2005; Whitehand, 1992). Previous studies have also found that urban spatial form has significant differences in thermal effects (Li et al., 2014; Rinner & Hussain, 2011; Zhou, Huang, & Cadenasso, 2011). For the land cover, LST is always higher in built-up areas, and lower in vegetated areas and water bodies (Li et al., 2016; Sun, Wu, & Tan, 2012). For the landscape diverse types, high patch density has the effect of reducing LST, whereas the high largest patch index and contagion index values may intensify LST (Chen, Yao, Sun, & Chen, 2014; Connors et al., 2013; Li et al., 2011). For building layout, high density and high-rise building have been proved that they can increase LST in the center of the city (Li, Zhang et al., 2012; Li, Zhou et al., 2012; Xiao et al., 2008; Yang, Su, Xia, Jin, & Ge, 2018), low building density and high floor area ratio tend to have a lower LST (Giridharan, Lau, & Ganesan, 2005; Guo et al., 2016; Yin, Yuan, Lu, Huang, & Liu, 2018).

However, some studies reached the paradoxical conclusions. Brian and Rodgers (2001) argued that the low-density residential contributed more heat than higher density habitations. Bourbia and Boucheriba (2010) found that the LST in high-density areas is low by comparing the ratio of building height and width in several residential areas with different densities in the day time. Taleghani et al. (2015) pointed out that compact urban spatial form can provide a comfortable microclimate in the Netherlands compared to other studied urban forms. Similarly, several researchers also concluded that the LST will increase with the increase of roof area and floor area ratio in compact urban blocks (Chun & Guhathakurta, 2017; Chun & Guldmann, 2014; Wei, Song, Wong, & Martin, 2016; Zhao, Fu, Liu, & Fu, 2011).

As noted above, the results of previous studies are contradictory in the quantitative evaluation of urban spatial form factors and LST, which means that the relationship between urban spatial form factors and LST remains under debate and has prevented consensus on how best to mitigate urban LST by urban planning methods. The reason for the opposite research conclusions lies in the different methods, spatial scales, regression models and climatic zones of the different studies. More importantly, in the current studies, most of the researches is carried out in plain cities, while mountainous cities are rarely analyzed. It is particularly necessary to further study the relationship between urban form factors and LST in high-density mountain cities and reveal the impact of urban spatial forms on LST to guide urban planning. Therefore, this paper needs to use multi-scale, multi-model and mountain city to study the relationship between urban spatial form factors and LST, and aims to 1) identify the influence of different spatial scales and regression models; 2) reveal the possible quantitative relationships urban forms and LST in mountainous city; 3) find out the urban spatial form factors that significantly affect LST.

## 2. Data and methods

### 2.1. Study area

Chongqing city in southwestern China is a typical mountainous city, in which there are high population and building densities. As the original area of Chongqing city, Yuzhong district has the highest population density than its other districts. Yuzhong district locates within the range of N 29°31′50″ – 29°34′20″ and E 106°28′50″ –106°35′10″, situated on the peninsula which was formed by the intersection of the

Yangtze River and its tributary, the Jialing River, with a land area of 18.35 square kilometers (Fig. 1a). Under the alternating action of river scour, Yuzhong district forms a unique intervalley denudation platform slope landform, and there are great topographical differences with a maximum elevation difference of 300.96 m (Fig. 1b and c). Yuzhong district contains 970,000 people with an average population density of 52,000 people per square kilometers, the average building density is 22.53 percent and road density reach 9.52 km per square kilometers. By the end of 2014, there were 2109 high-rise buildings over 24 m, of which 407 are super high-rise buildings over 100 m (Fig. 1d). Therefore, it is one of the cities with the highest density and intensity of high-rise buildings in China. The climate is defined as a typical hot and humid climate, and its static wind speeds are less than three meters per second (Yong, Wen, & Zhao, 2004) throughout the year. Combined with high density and poor ventilation conditions, Yuzhong district has a worse thermal environment than other districts, as well as other cities in China (Cai & Han, 2018; Han, Yan et al., 2012; Han, Ye, & Sun, 2014; Han, Zhao, Yan, & Ye, 2012).

### 2.2. Data sources and pre-processing

Cloud-free Landsat8 OLI_TIRS remote-sensing images in summer and winter daytime were downloaded from the website (http://www.gscloud.cn) (Table 1). Demographic data in these communities in 2014 were collected from the Bureau of Statistics of the Yuzhong district. The current land use map (2014) and building map (2014), as well as the regulatory plans (2010) covering the entire district were collected from the Department of Housing and Urban-Rural Development of the Yuzhong government. The digital elevation model (DEM) was created from the digital topographic maps with a scale of 1: 500.

### 2.3. Methods

This study included the following four steps to processing and analysis the data (Fig. 2): (1) Collect data and retrieve LST; (2) Initialize spatial scales and calculate urban spatial form factors; (3) Pearson correlation analysis and select the optimal spatial scale; (4) Multiple regression model analysis.

#### 2.3.1. Retrieve land surface temperature

In this study, LST was retrieved by using the radiation transfer equation (RTE) (Weng, 2009; Yue & Tan, 2007) and the formula is as follows:

$$L_\lambda = [\varepsilon B(T_S) + (1-\varepsilon)L\downarrow]\tau + L\uparrow \quad (1)$$

where $L_\lambda$ is the thermal infrared radiation brightness value received by the satellite sensor, $\varepsilon$ is surface emissivity. Since OLI Band10 has an approximate spectral range with the thermal infrared band of TM/ETM, this paper calculated ε using the NDVI threshold method (Sobrino, Jiménez-Muñoz, & Paolini, 2004) as a reference.

$$\varepsilon = 0.004P_V + 0.986 \quad (2)$$

where $P_v$ is the vegetation fraction, which can be calculated using the following formula:

$$P_V = \frac{NDVI - NDVI_{soil}}{NDVI_{veg} - NDVI_{soil}} \quad (3)$$

**Table 1**
The information of Landsat 8 remote-sensing images in this study.

| Season | Time | Path | Row |
|---|---|---|---|
| Summer | 11:26 AM, 6 August, 2014 | 128 | 39 |
| Winter | 11:23 AM, 2 December, 2013 | 127 | 40 |

$$NDVI = \frac{NIR - R}{NIR + R} \quad (4)$$

where NDVI is the normalized vegetation index, $NDVI_{soil}$ is the value of the area completely covered by bare soil or non-vegetated, and $NDVI_{veg}$ is the value of the area completely covered by vegetation. As a matter of experience (Qin, Li, Xu, Chen, & Liu, 2004), $NDVI_{soil}$ is 0.05 and $NDVI_{veg}$ is 0.7. When NDVI is more than 0.7, the value of $P_v$ is 1, when NDVI is less than 0.05, the value of $P_v$ is 0. NIR is the near-infrared band (band 5), R is the red band (band 4) in Landsat 8.

The atmospheric downward radiance $L\downarrow$, upward radiance $L\uparrow$, and transmissivity $\tau$ are obtained from the NASA website (http://atmcorr.gsfc.nasa.gov/). $T_s$ is the surface true temperature (K), $B(T_s)$ is the black body thermal radiance, and it can be calculated as follows:

$$B(T_s) = \frac{C_1}{\lambda^5(e^{C_2/\lambda T_s} - 1)} \quad (5)$$

$C_1$ and $C_2$ are radiation constants with values of $1.19104356 \times 10^8$ ($Wm^{-2}sr^{-1}\mu m^4$) and $1.4387685 \times 10^4$ (μm K) respectively, and λ is the wavelength (μm). $T_S$ can be expressed as follows:

$$T_S = \frac{K_2}{ln(K_1/B(T_S) + 1)} \quad (6)$$

For the Landsat 8 TIRS Band 10 data, $K_1 = 774.89\ Wm^{-2}sr^{-1}\mu m^{-1}$ and $K_2 = 1321.08$ K.

$$LST = T_S - 273.15 \quad (7)$$

#### 2.3.2. Initialize spatial scales and calculate urban spatial form factors

Spatial patterns, processes, spatial-temporal distribution and the mutual coupling of spatial objects are influenced by the spatial scale (Chun & Guldmann, 2014). In order to find out the optimal spatial scale in this study area. We select ten spatial grid scales at the intervals of 60 m: 30 m, 90 m, 150 m, 210 m, 270 m, 330 m, 390 m, 450 m, 510 m and 570 m. In addition, two other spatial grid scales (1000 m and 2000 m) are also selected as tentative scales, as they represent fewer samples (Fig. 3). The mean values of each urban form factors and LST for every grid on each spatial scale are extracted using the spatial analyst tools in ArcGIS software (version 10.3).

(a. 30 m gird size; b. 90 m grid size; c. 150 m gird size; d. 570 m grid size.)

According to previous studies (Cai, Han, & Chen, 2018; Chun & Guhathakurta, 2017; Guo et al., 2016; Sharifi, 2019; Stewart & Oke, 2012; Stewart, 2011; Wei et al., 2016; Yin et al., 2018), several common urban spatial factors are widely used in urban thermal environment studies, such as sky view factor (SVF), building density (BD) and floor area ratio (FAR). Thus, the above three factors are also selected in this study. Since mountain city with a great undulate topography and unique building spatial form, urban surface roughness (USR) were also selected. Moreover, as the transportation network in mountain cities is different from plain cities, the road surface area density (RSD) is selected to reflect this difference. The definition and calculation formula of urban spatial form factors are in Table 2.

#### 2.3.3. Pearson correlation analysis and select the optimal spatial scale

SPSS software is then used to analyze the Pearson correlation between urban spatial form factors and the LST on twelve spatial scales. The best spatial scale is found by comparing the Pearson correlation coefficients.

#### 2.3.4. Multiple regression model analysis

The ordinary least square (OLS) and three spatial regression models (space lag model, spatial error model and general space model) are used to analyze the impacts of urban form factors on LST in GeoDaSpace1.0. The ordinary least squares (OLS) model is based on an assumption of independence, and its result ignores the spatial effect between spatial things (Li, Zhao, Miaomiao, & Wang, 2010). However, due to heat

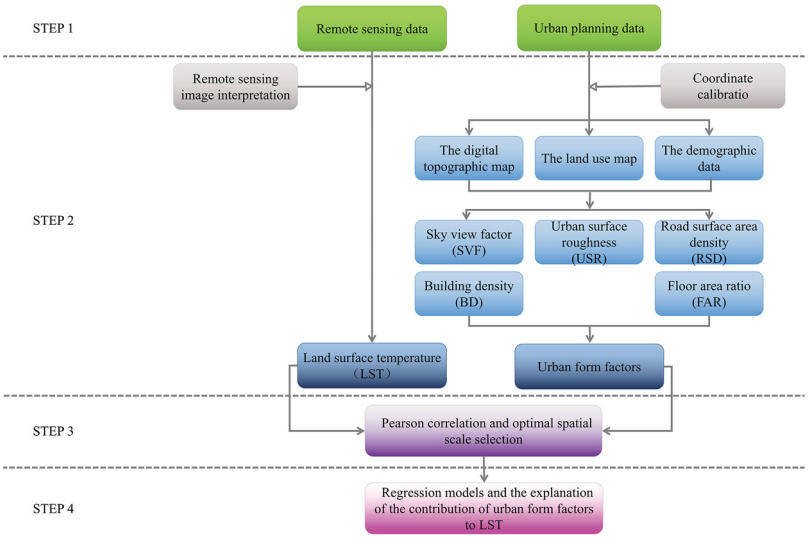



**Fig. 2.** Study framework.

conduction, convection and radiation, the land surface and airflow provide conditions for heat movement, so LST is constantly changing in space (Kim et al., 2016), and this phenomenon will lead to the autocorrelation of LST in space. Therefore, we use three spatial regression models to deal with the problem of spatial interaction.

First, the OLS model is used to test the relationship between urban form factors and LST using the equation:

$$y = \alpha + X\beta + u \tag{8}$$

Where $\alpha$ is constant term; $y$ is the dependent variable, which refers to LST; $X$ is the explanatory variable, which refers to the urban forms; $\beta$ is the regression coefficient, and $u$ is an error term.

Moran's I (Moran, 1950) is then calculated to assess whether the OLS residuals are related to spatial autocorrelation using the equation:

$$I = \frac{n}{\sum_i \sum_j w_{ij}} \frac{\sum_i \sum_j w_{ij}(x_i - \bar{x})(x_j - \bar{x})}{\sum_i (x_i - \bar{x})^2} \tag{9}$$

Where $x_i$ and $x_j$ are the values of LST observed at locations $i$ and $j$; $\bar{x}$ is the mean of the $x$; and $W_{ij}$ is a measure of the spatial relationship between locations $i$ and $j$. The value of Moran's I varies between -1 and 1, with values close to 0 indicating little spatial autocorrelation. If the value is found to be significant, then a spatial lag model (SLM) need to be tested to address the spillover effect, which takes the following form:

$$y = \alpha + \rho W_y + X\beta + \varepsilon,\ \varepsilon \sim N(0, \sigma^2 I_n) \tag{10}$$

Where $\rho$ is a spatial lag term; $W$ is the spatial weight matrix that contains non-zero element $W_{ij}$ when observation $i$ and $j$ are neighbors and zero elements otherwise, and $W_y$ represents the average value of $y$ at neighboring locations (Lesage & Pace, 2014). The Lagrange multiplier (LM) test can determine whether the $y$ values are affected by unobserved variables with spatial effects in the model. If the test is positive, the spatial error term is modified by means of the spatial error model (SEM) (Eq. (11)) to reduce the residual spatial effects. In addition, when both the SLM and the SEM models are ineffective in reducing the spatial effects, the general spatial model (GSM) (Eq. (12)) is appropriately considered (Chun & Guhathakurta, 2017; Lesage & Pace, 2014). The formulas for the SEM and GSM models are as follows:

$$y = \alpha + \rho W y + (\lambda W_u + \varepsilon),\ \varepsilon \sim N(0, \sigma^2 I_n) \tag{11}$$

$$y = \alpha + \rho W_1 y + X\beta + (\lambda W_2 u + \varepsilon),\ \varepsilon \sim N(0, \sigma^2 I_n) \tag{12}$$

Where $\lambda$ is a spatial error term coefficient, $W_1$ is the spatial weight matrix used for LST, and $W_2$ is the spatial weight matrix used for the error term.

## 3. Results

### 3.1. The distribution of LST

The LST ranges from 22.05 °C to 43.79 °C, and there are great spatial distribution differences (Fig. 4). The low LST located in the central region such as Eling, where there has a great topographical difference and difficult to construct, lots of green spaces has appeared in those regions. The high LST is distributed in the eastern and western regions, such as Lianglukou, Daping, Shiyoulu, Qixinggang and Daxigou. Where there are high-density urban construction areas and have few green spaces, the urban spatial form is dominated by compact high-rise buildings. Which results the heat energies accumulated in those areas and has a higher LST.

### 3.2. Optimal spatial scale

Pearson correlation coefficients between the five urban spatial form factors and LST on all twelve spatial scales are shown in Table 3. In summer daytime, most of their correlation coefficients increase with the

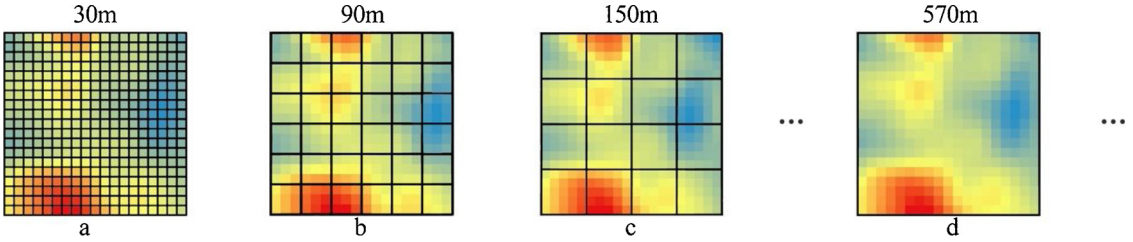
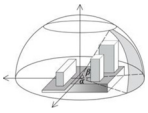
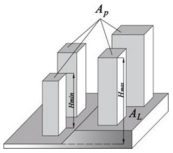
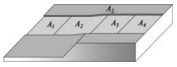
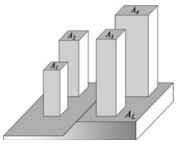
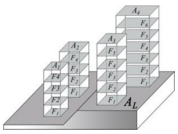



**Fig. 3.** The process of spatial upscaling.

**Table 2**
The definition and calculation of the formula for urban spatial form factors.

| Factor | Definition | Formula | Illustrate |
|---|---|---|---|
| Sky view factor (SVF) | The ratio between the radiation received by a planar surface and the entire hemispheric radiating environment (Watson & Johnson, 1987). | $SVF = 1 - \sum_{i=1}^{N} sin^2\beta_i \left(\frac{\alpha_i}{360^0}\right)$ $N$ is the total number of the angle elements of the obstacles in the hemispheric environment, and $\alpha_i$ and $\beta_i$ reflect the elevation and azimuth angles of the angle element $i$, respectively (Matuschek & Matzarakis, 2010). |  |
| Urban surface roughness (USR) | The relative height difference of urban surface within a certain region. | $USR = (H_{max} - H_{min}) \times \left(1 - \frac{A_P}{A_L}\right) \times 500$ $H_{max}$ and $H_{min}$ are the highest and lowest elevations of a region, respectively, $A_P$ and $A_L$ are the flat area and total land area of the region, respectively. |  |
| Road surface area density (RSD) | The ratio of traffic road surface area to a plot area. | $RSD = \frac{\sum_{N}^{i=1} N \times A_i}{A_L}$ $A_i$ is the area of the raster cell, and $N$ is the number of raster cells, $A_L$ is the area of the land lot. |  |
| Building density (BD) | The ratio of building base area to plot area. | $BD = \frac{\sum_{N}^{i=1} A_i}{A_L}$ $A_i$ is the base area of buildings in a land lot, and $A_L$ is the area of the land lot. |  |
| Floor area ratio (FAR) | The ratio of the total floor area to the land area of a land lot. | $FAR = \frac{\sum_{N}^{i=1} A_i \times F_i}{A_L}$ $A_i$ is the base area of construction building in a land lot, $F_i$ is the number of building floors, and $A_L$ is the area of the land lot. |  |

spatial scales and reach maximum values at 510 m, then decrease gradually. There is a significant positive correlation between LST and SVF, followed by RSD, USR and BD. While FAR has no significant relationship with LST. With the increasing spatial scale, each grid contains more land-use types. Therefore, the correlation coefficients between urban spatial form factors and LST are not significant when the spatial scale is more than 510 m. Consequently, 510 m is considered as the optimal spatial scale to analyze their relationships.

### 3.3. Correlation between urban spatial form factors and LST

#### 3.3.1. Significant positive correlation between urban spatial form factors and LST

There is a significant positive correlation between SVF, USR, RSD, BD and LST (Table 3), which implies that LST gradually increases with those urban spatial form factors values.

For SVF, the spatial distribution of SVF is strongly dependent upon urban form conditions. Taking the Chongqing railway station in Caiyuanba as an example, there is almost no vegetation in the square and it is covered by impervious concrete and asphalt (Fig. 5). One sampling line from the northwest to the southeast shows a trend of LST accompanying a trend of SVF (high-high trend). Exposed to solar radiation, the low heat capacity of impervious land surfaces increases LST rapidly in such a large open space. At the southeast end of the section, LST reasonably decreases due to the cooling effect of a body of water (Yangtze River), even though there is still a high SVF in that area (Cai & Han, 2018). In contrast, it is easy to see a low-low trend of SVF and LST in section B-B' in a narrow space in Qixinggang (Fig. 6). Low SVF and

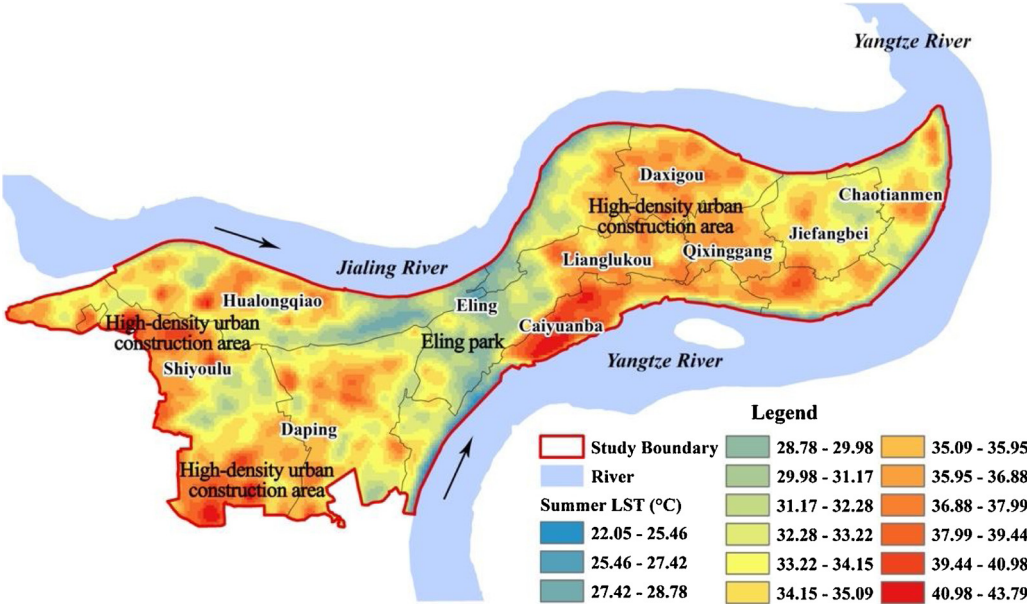



**Fig. 4.** The distribution of land surface temperature in summer daytime.

**Table 3**
Pearson correlation coefficients between urban spatial form factors and LST.

| Scale | Count | Summer | | | | | Winter | | | | | Legend |
|---|---|---|---|---|---|---|---|---|---|---|---|---|
| | | SVF | USR | RSD | BD | FAR | SVF | USR | RSD | BD | FAR | |
| 30m | 19674 | 0.015* | -0.12** | -0.09* | 0.047** | -0.004 | .035** | -.110** | .036** | .047** | -0.004 | >0.35 |
| 90m | 2319 | 0.194** | -0.071** | -0.069* | 0.067** | 0.003 | .058** | -.152** | .071** | .074** | -0.004 | 0.3 |
| 150m | 878 | 0.304** | -0.02 | -0.011 | 0.093** | 0.019 | .076* | -.195** | .084* | .080* | -0.012 | 0.25 |
| 210m | 477 | 0.383** | 0.06 | 0.143* | 0.112* | 0.043 | .104* | -.224** | 0.084 | 0.085 | -0.017 | 0.2 |
| 270m | 310 | 0.369** | 0.096 | 0.221* | 0.134* | 0.051 | .130* | -.268** | 0.096 | .113* | 0.004 | 0.15 |
| 330m | 212 | 0.403** | 0.118 | 0.251* | 0.159* | 0.061 | 0.091 | -.187** | 0.104 | .137* | 0 | 0.1 |
| 390m | 159 | 0.368** | 0.139 | 0.288* | 0.184* | 0.104 | 0.148 | -.277** | 0.07 | 0.085 | -0.054 | 0.05 |
| 450m | 121 | 0.378** | 0.143 | 0.358* | 0.187* | 0.101 | 0.077 | -.247** | .184* | 0.074 | -0.041 | 0 |
| 510m | 104 | 0.411** | 0.214* | 0.432* | 0.212* | 0.145 | 0.079 | -.232* | 0.12 | 0.088 | 0.009 | -0.05 |
| 570m | 78 | 0.266* | 0.049 | 0.345* | 0.143 | 0.048 | 0.166 | -.237* | -0.005 | 0.094 | 0.034 | -0.1 |
| 1000m | 34 | 0.237 | 0.135 | 0.48* | 0.172 | 0.097 | 0.044 | -.363* | -0.012 | -0.017 | -0.12 | -0.15 |
| 2000m | 14 | 0.2 | 0.167 | 0.517 | 0.21 | 0.141 | 0.419 | -0.411 | -0.055 | 0.306 | 0.12 | <0.2 |

**P (2-tailed) < 0.01.
*P (2-tailed) < 0.05.

low LST are consistently seen in narrow streets and courtyards surrounded by high-rise buildings. In high-rise and high-density areas, the high buildings always play the role of a barrier against solar radiation and create large shadowed areas in narrow streets and courtyards. Heat exchange occurs between the area exposed to the sun and the shadowed area because of temperature gradients, which results in street canyon wind through the streets (Chen, 2008). Therefore, a significant positive correlation is get between SVF and LST, which is similar to that observed in the research of Oke (1987), Unger (2009) and Guo et al. (2016).

For USR, land surface roughness measures the fluctuation of natural land surface and buildings. It is well known that wind is conducive to promoting heat exchange and reducing LST. However, when the wind flows through a city and touches the urban surface, the speed and direction of the wind current will be adjusted, and most wind currents rise up against the windward side and rarely enter the urban canopy layer. In an urbanized area with high-density construction, the obstruction effect of the buildings on wind currents becomes more and more obvious. Therefore, it is easy to understand that high levels of roughness lead to high LST.

For RSD, the total area of urban roads with widths over 7 m is approximately 4.54 square kilometers, 24.74 percent of the total study area. Almost all roads are made of impervious materials such as asphalt and concrete, which have high absorption rates and thermal conductivity. Road surfaces directly absorb solar radiant energy during the day, causing heat to accumulate on their surfaces, and the dissipating of this heat causes the road surface temperature to rise significantly (Lo et al., 1997). In addition, vehicles drove on the road emit hot exhaust gas and transmit heat to near the roads' surfaces, so that the road networks like electric stove wires that keep heating in the city.

For BD, BD is the proportion of the area occupied by buildings within a piece of land, and it also indirectly reflects the amount of impermeable surface and the distance between buildings. In general, high-density areas are often composed of dense buildings with small distances (narrow streets) between buildings. The wind speed in narrow streets will be decreased by buildings surrounding area, therefore air ventilation efficiency will be reduced in the area, resulting in an increase of the regional LST. In addition, there are almost no enough free public spaces such as parks featuring vegetation and squares, which is not conducive to LST reduction and evacuation. In contrast, when the number of buildings is small and the distribution of buildings is sparse, this is conducive to the exchange of hot and cold air, the air ventilation efficiency in the area is high, and the LST is relatively low. Therefore, there is a significant positive correlation between BD and LST (Fig. 7).

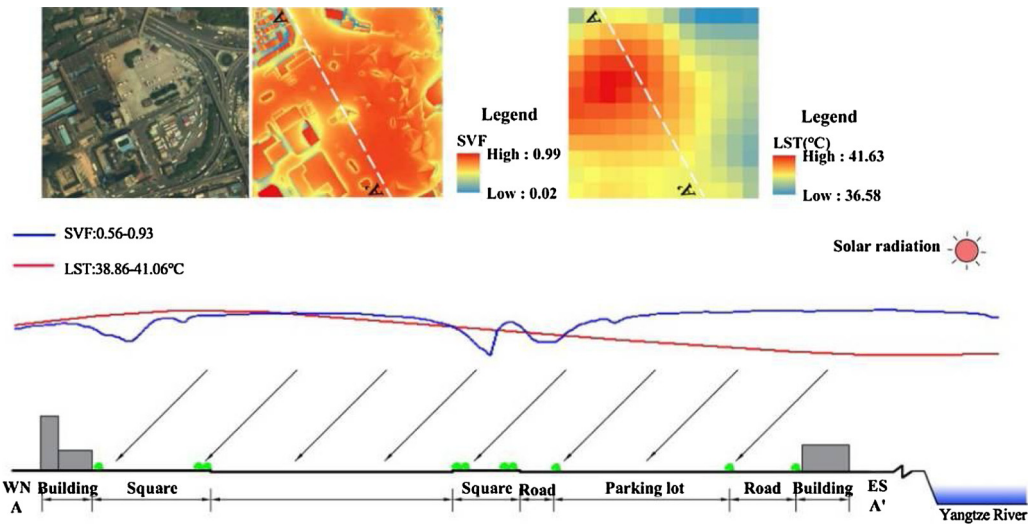



**Fig. 5.** The high-high trend of SVF and LST along a section line through big open square.

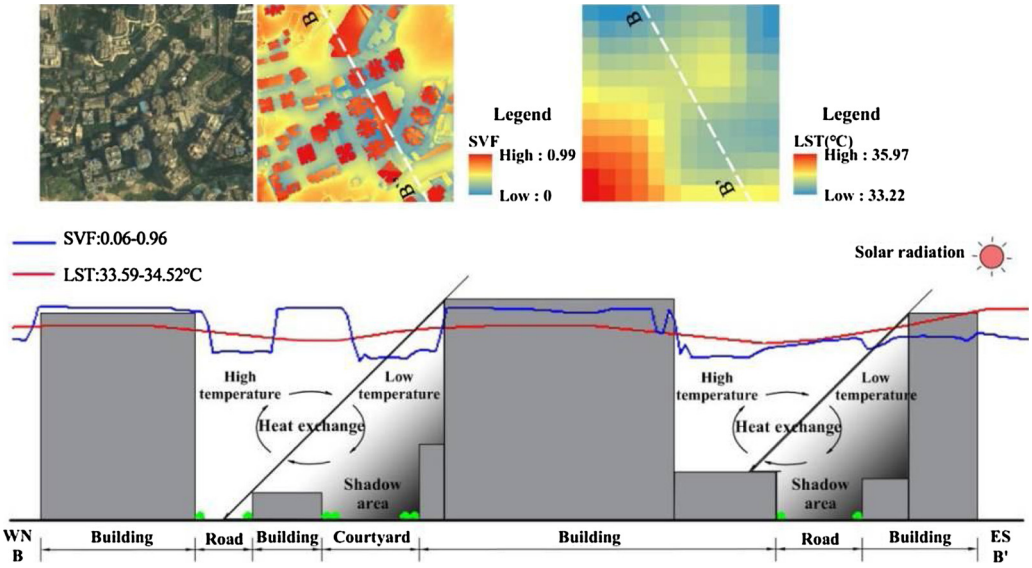



**Fig. 6.** The low-low trend of SVF on LST along a section line through narrow space.

*3.3.2. Not significant correlation between FAR and LST*

Even though FAR have a positive relationship with LST, this correlation is not significant (Table 3). FAR reflects the construction intensity of a land lot. In general, a high construction intensity area could have more buildings and contain more populations. Those areas have more human activities and anthropogenic heat release, and have a high LST. However, as the FAR is based on a land lot, the land lot with different building spatial forms could have a same FAR value, such as compact mid-rise and open high-rise. Where, open high-rise has more open spaces and lower LST than compact mid-rise (Cai et al., 2019). Moreover, the high-rise buildings can provide more building shadows and reduce the solar energy reaches to the land surface, which will make the relationship between FAR and LST not significant, even they have a positive relationship in some studies (Cai et al., 2018).

### 3.4. Regression models between urban spatial form factors and LST

Several regression models were applied to find the contribution of urban spatial form factors on LST. Since FAR has no significant correlation with LST, and it has multicollinearity with other factors like SVF. Therefore, FAR is excluded from the regression models. The results show that the goodness of fit (R squared) increased from OLS (0.24), to SLM (0.69), to SEM (0.76), and to GSM (0.80) (Table 4). OLS is a simple and linear regression model, and it can not eliminate the parameters with spatial autocorrelations (Yin et al., 2018). As the Moran's I value for LST reaches 0.56 ($P < 0.01$) in this study, OLS did not work well. The spatial regression model (SLM, SEM and GSM) considered the spatial correlations, and they work better than OLS. However, there should be noted that only SVF performs as a stable parameter and have a significant positive impact on LST in the four regression models. Due to the spatial spillover (significant LM-Lag) and spatial heterogeneity effect, USR, RSD and BD did not stable and have a significant contribution to LST. Which is inconsistent with other relevant studies (Chun & Guhathakurta, 2017; Chun & Guldmann, 2018).

## 4. Discussion

### 4.1. Influence of topography on LST

Chongqing city is a mountain city, and it has an intervalley denudation platform slope landform and great topographical differences, which may have an impact on the urban thermal environment. Therefore, we analyzed the influence of topography factors on LST, such as slope and aspect. The results showed that slope has a significant negative relationship with LST in summer daytime (-0.26**, $P < 0.01$), and this correlation decreased to -0.162** ($P < 0.01$) in winter daytime. The plain land with small slope value usually selects as construction zone, building and impervious surface are concentrated in those areas. On the contrary, the land with high slope value are difficult to construct, and those areas always remain as green spaces, they have a lower LST than plain areas.

In summer, the LST in various aspect decreased from southwest (43.9 ℃), to south (43.8 ℃), to east (43.7 ℃), to east (43.4 ℃), to southeast (43.2 ℃), to northeast (43.2 ℃), to northwest (43.0 ℃), and to north (42.6 ℃) (Fig. 8a). In winter, the LST decreased from south (15.6 ℃), to southeast (15.4 ℃), to southwest (15.3 ℃), to east (15.2 ℃), to west (14.9 ℃), to northeast (14.6 ℃), to northwest (14.5 ℃), and to north (14.3 ℃) (Fig. 8b). Which illustrated that the south aspect

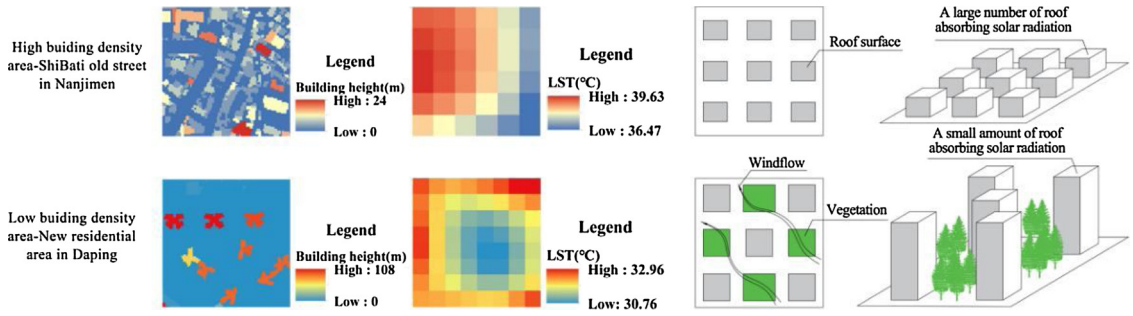



**Fig. 7.** Impacts of building densities on LST.

**Table 4**
The four regression models between urban form factors and LST.

| Independent variables | Dependent variable: LST | | | |
|---|---|---|---|---|
| | OLS | SLM | SEM | GSM |
| Constant | 31.77** | 3.26* | 32.06** | −3.39 |
| | (59.68) | (1.99) | (31.13) | (-0.63) |
| Sky view factor (SVF) | 0.02** | 0.02** | 0.01** | 0.01** |
| | (4.81) | (5.03) | (3.49) | (3.05) |
| Urban surface roughness (USR) | $-2.79 \times 10^{-4}$* | $-1.51 \times 10^{-4}$* | $-0.50 \times 10^{-4}$ | $-0.96 \times 10^{-4}$ |
| | (-2.42) | (-2.05) | (-0.77) | (-1.46) |
| Road surface area density (RSD) | $-0.04 \times 10^{-4}$ | $0.05 \times 10^{-4}$ | $0.03 \times 10^{-4}$ | $0.09 \times 10^{-4}$ |
| | (-0.26) | (0.47) | (1.74) | (1.15) |
| Building density (BD) | $-7.17 \times 10^{-4}$ | $3.04 \times 10^{-4}$ | $8.45 \times 10^{-4}$ | $8.21 \times 10^{-4}$ |
| | (-0.37) | (0.24) | (0.93) | (0.82) |
| Spatial lag term (ρ) | — | 0.84** | — | 1.06** |
| | | (17.46) | | (6.56) |
| Spatial error term (λ) | — | — | 0.87** | −0.10 |
| | | | (21.29) | (-0.38) |
| $R^2$ | 0.24 | 0.69 | 0.76 | 0.80 |
| Moran's I | 0.56 | | | |
| LM-Lag | | 58.13** | | |
| LM-Error | | | 52.28** | |

() t-stat.
**P < 0.01;
*P < 0.05;

tends to have a higher LST, and the north aspect tends to have a lower LST both in summer and winter daytimes. The south aspect is directly facing to the sun, while the north aspect is back to the sun. Which means the south aspect can receive more solar energies than north aspect, and the south area has fewer shadows from building or mountain, the significant negative correlation between shadows and LST also identified those effect (-0.307, P < 0.05). With the rise of shadows in the winter time, the correlation between shadows and LST has also increased (-0.633, P < 0.01).

In this study area, it has 26.5 percent land with a slope above 15 degrees, and about 40 percent area faced to the north (northwest, north and northeast). This means that the influence of topography on LST was cover a large part of the study area. Thus, it is necessary to consider those impacts on mountainous city studies.

### 4.2. The unique urban spatial form in a mountainous city

As a mountainous city, the composition of the underlying urban surface is very complicated (Table 5). There is almost no flat land in this study area, which has a difference of elevation more than 200 m. The profiles of a mountainous city change with the relief of the terrain. What's more, due to the limitations of the terrain, there are many rivers and dispersive lawns. Additionally, the roads are narrow and curved, which is quite different from those of plain cities. With the continuous renewal and development of urban construction, the differences in the shape of the buildings, the height of the buildings and the colour of the buildings are becoming more and more obvious, which makes the landscape more diverse on the underlying surface. In a plain city, the underlying surface is flat and even, the architectural layout of the city is often relatively homogeneous, and the buildings have a similar shape, height and colour. Moreover, most of the water bodies are made of lakes, and the centralized parks and meadows make up the green spaces. This may be one of the reasons why our research results are not as clear as those from previous studies in other cities (Chun & Guhathakurta, 2017; Chun & Guldmann, 2018). In addition, Cai and Han (2018) found that water bodies have a significant impact on the relationships between the urban form factors and LST, particularly at a distance from the riverside of less than 250 m. Hence, this paper tries to eliminate those samples within 250 m of the riverside in the 510 m' spatial scale and recalculate the four models using the remainder of the samples. The result shows that the $R^2$ value increases from 0.69 to 0.74 in the SLM model; however, the $R^2$ value of the other three models does not improve significantly. This implies that the cooling effect of the body of water may have a modest degree of influence on the regression models.

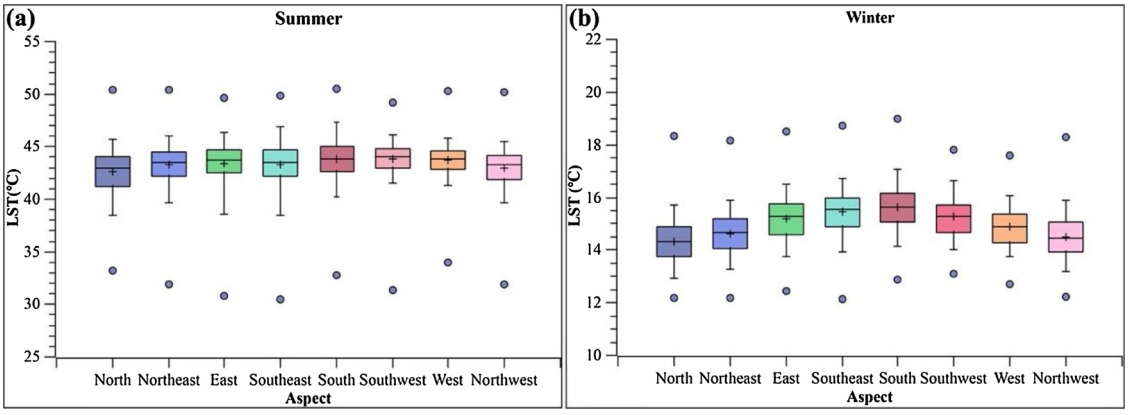
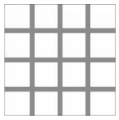
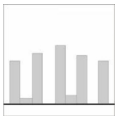
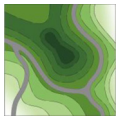
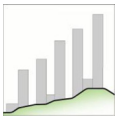
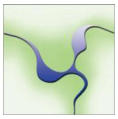



**Fig. 8.** The box plots of LST in eight aspects: (a) summer daytime, (b) winter daytime.

**Table 5**
Comparison of underlying surface between mountainous city and plain city.

| Type | Roads | Buildings | Profiles | Water bodies | Green spaces |
|---|---|---|---|---|---|
| City in plain |  Regular networks |  Monotonous building layout |  Flat ground |  Lakes |  Centralized parks, meadows |
| City in mountain |  Irregular networks |  Diverse building layout |  Coarse ground |  Rivers |  Dispersive lawn |

### 4.3. Limitations

In this study, we only focus on the contribution of physical construction factors (urban spatial form) to LST. It is well known that LST is a consequence of absorbed solar radiation and anthropogenic heat sources with a synthesized influence of many factors. Many studies show that anthropogenic heat sources play an important role in urban area warming (Fang et al., 2016). Anthropogenic heat sources are intrinsic energy sources that promote LST rises, including industrial activities, building energy consumption, automobile exhaust and human metabolism (Sailor & Lu, 2004), which are emitted into the atmosphere and transmitted in urban spaces, causing a change in the heat transfer mechanism. What's more, this paper simplifies the shape of the buildings, treats them into three-dimensional cubes, and ignores the differences in the roof, which may have some influence on the results of the study. Moreover, only the LST derived from remote sensing images cannot directly reflect the level of heat stress of human bodies and this paper does not verify the relationships using air temperature because synchronous measurements are difficult in the big urban area. In addition, many studies show that water bodies can release heat to the surrounding air because of the high heat capacity at night or in winter (Chun & Guhathakurta, 2017; Moyer & Hawkins, 2017; Steeneveld, Koopmans, Heusinkveld, & Theeuwes, 2014), which will be considered in future studies.

In future work, it is necessary to conduct a comparative study among several mountainous cities and find the common relationships between urban spatial form factors and LST. Of course, more factors should be considered, such as the materials, colours, shapes and roofs of buildings and anthropogenic heat sources. In addition, it is worth studying on relationships between urban spatial forms and LST based on time-series image data in the four seasons. Nonlinear regression models can also be used to analyze the relationship between urban spatial form and urban heat island and provide more powerfully prediction.

## 5. Conclusions

In this study, we found that the spatial scale influences the correlations between urban spatial form factors and LST, and the optimal spatial scale changed over the season. Therefore, the spatial scale should be considered in other studies. There is a significant positive correlation between SVF, USR, RSD, BD and LST, and the positive correlation between FAR and LST is not significant. FAR has also multicollinearity with other factors. Even though the spatial regression models (SLM, SEM, GSM) working better than the OLS model, it should be noted that some urban spatial form factors did not show a significant contribution to LST in the spatial models, due to their spatial spillover and spatial heterogeneity effect. Besides the spatial effect, the unique topography of mountainous city also has an impact on the urban thermal environment, such as the slope, aspect and underlying surface. Which implies that the thermal environment in mountainous cities is more complicated than plain cities, the planners should also consider the topography impact and using different methods to mitigate UHI, and making the mountainous cities cope with climate change.

## Funding

This study is supported by the National Natural Science Foundation of China (Grant numbers 51778077, 51978091).

## Appendix A

Table A1

**Table A1**
The meanings of the abbreviations in the text.

| Abbreviation | Meaning | Abbreviation | Meaning |
|---|---|---|---|
| LST | land surface temperature | UHI | urban heat island |
| SUHI | surface urban heat island | SVF | sky view factor |
| USR | urban surface roughness | BD | building density |
| RSD | road surface area density | FAR | floor area ratio |
| SEM | spatial error model | RTE | radiation transfer equation |
| NDVI | normalized difference vegetation index | SLM | spatial lag model |
| OLS | ordinary least square | GSM | general spatial model |

## References


Bourbia, F., & Boucheriba, F. (2010). Impact of street design on urban microclimate for semi arid climate (Constantine). *Renewable Energy, 35*(2), 343–347. https://doi.org/10.1016/j.renene.2009.07.017.

Brian, S., Jr., & Rodgers, M. O. (2001). Urban form and thermal efficiency: How the design of cities influences the urban heat island effect. *Journal of the American Planning Association, 67*(2), 186–198. https://doi.org/10.1080/01944360108976228.

Cai, Z., & Han, G. F. (2018). The surface thermal environment effect of spatial forms of mountain cities—Based on the perspective of LCZ. *Journal of Mountain Research, 36*(04), 617–627 In Chinese.

Cai, Z., Han, G., & Chen, M. (2018). Do water bodies play an important role in the relationship between urban form and land surface temperature. *Sustainable Cities and Society, 39*, 487–498. https://doi.org/10.1016/j.scs.2018.02.033.

Cai, Z., Tang, Y., Chen, K., & Han, G. (2019). Assessing the heat vulnerability of different local climate zones in the old areas of a Chinese megacity. *Sustainability, 11*(7), 2032. https://doi.org/10.3390/su11072032.

Chang, C. R., Li, M. H., & Chang, S. D. (2007). A preliminary study on the local cool-island intensity of Taipei city parks. *Landscape and Urban Planning, 80*(4), 386–395. https://doi.org/10.1016/j.landurbplan.2006.09.005.

Chen, F. (2008). Research on wind environment of high-rise buildings. *Architectural Journal, 2*, 72–77 In Chinese.

Chen, A., Yao, L., Sun, R., & Chen, L. (2014). How many metrics are required to identify the effects of the landscape pattern on land surface temperature? *Ecological Indicators, 45*, 424–433. https://doi.org/10.1016/j.ecolind.2014.05.002.

Chen, X., Zhao, H., Li, P., & Yin, Z. (2006). Remote sensing image-based analysis of the relationship between urban heat island and land use/cover changes. *Remote Sensing of Environment, 104*(2), 133–146. https://doi.org/10.1016/j.rse.2005.11.016.

Chun, B., & Guhathakurta, S. (2017). Daytime and nighttime urban heat islands statistical models for Atlanta. *Environment and Planning B-planning and Design, 44*(2), 308–327. https://doi.org/10.1177/0265813515624685.

Chun, B., & Guldmann, J. (2018). Impact of greening on the urban heat island: Seasonal variations and mitigation strategies. *Computers, Environment and Urban Systems, 71*, 165–176. https://doi.org/10.1016/j.compenvurbsys.2018.05.006.

Chun, B., & Guldmann, J. M. (2014). Spatial statistical analysis and simulation of the urban heat island in high-density central cities. *Landscape and Urban Planning, 125*, 76–88. https://doi.org/10.1016/j.landurbplan.2014.01.016.

Connors, J. P., Galletti, C. S., & Chow, W. T. (2013). Landscape configuration and urban heat island effects: assessing the relationship between landscape characteristics and land surface temperature in Phoenix, Arizona. *Landscape Ecology, 28*(2), 271–283. https://doi.org/10.1007/s10980-012-9833-1.

Conzen, M. P. (2001). The study of urban form in the United States. *Urban Morphology, 5*(1), 3–14. http://urbanmorphology.org/pdf/conzen2001.pdf.

Coseo, P., & Larsen, L. (2014). How factors of land use/land cover, building configuration, and adjacent heat sources and sinks explain urban heat islands in Chicago. *Landscape and Urban Planning, 125*, 117–129. https://doi.org/10.1016/j.landurbplan.2014.02.019.

Debbage, N., & Shepherd, J. M. (2015). The urban heat island effect and city contiguity. *Computers, Environment and Urban Systems, 54*, 181–194. https://doi.org/10.1016/j.compenvurbsys.2015.08.002.

Fang, C., Wang, S., & Li, G. (2015). Changing urban forms and carbon dioxide emissions in China: A case study of 30 provincial capital cities. *Applied Energy, 158*, 519–531. https://doi.org/10.1016/j.apenergy.2015.08.095.

Fang, Y. B., Zhan, W. F., Huang, F., Gao, L., Quan, J. L., & Zou, Z. X. (2016). Time-varying regularity of urban heat islands on the surface of the Yangtze River Delta urban agglomeration. *Progress in Earth Science, 32*(2), 187–198 In Chinese.

Feyisa, G. L., Dons, K., & Meilby, H. (2014). Efficiency of parks in mitigating urban heat island effect: An example from Addis Ababa. *Landscape and Urban Planning, 123*, 87–95. https://doi.org/10.1016/j.landurbplan.2013.12.008.

Giridharan, R., Lau, S. S. Y., & Ganesan, S. (2005). Nocturnal heat island effect in urban residential developments of Hong kong. *Energy and Buildings, 37*(9), 964–971. https://doi.org/10.1016/j.enbuild.2004.12.005.

Guo, G., Zhou, X., Wu, Z., Xiao, R., & Chen, Y. (2016). Characterizing the impact of urban morphology heterogeneity on land surface temperature in Guangzhou, China. *Environmental Modelling and Software, 84*, 427–439. https://doi.org/10.1016/j.envsoft.2016.06.021.

Han, G. F., Ye, L., & Sun, Z. W. (2014). Influence of aspect on land surface temperature in mountain city: A case study in central area of Chongqing City. *Acta Ecologica Sinica, 34*(14), 4017–4024 In Chinese.

Han, G. F., Yan, W. T., Zhao, K., & Ye, L. (2012). Spatial-temporal changes of surface heat island in the central area of Chongqing over the past 20 years. *Research of Environmental Sciences, 25*(6), 615–621 In Chinese.

Han, G. F., Zhao, K., Yan, W. T., & Ye, L. (2012). Multi-gradients of land surface temperature in mountainous cities with rapid urbanization: A case study in central area of Chongqing City. *Chinese Journal of Applied Ecology, 23*(06), 1655–1662 In Chinese.

Hebbert, M. (2014). Climatology for city planning in historical perspective. *Urban Climate, 10*, 204–215. https://doi.org/10.1016/j.uclim.2014.07.001.

Howard, L. (1833). *The climate of London deduced from meteorological observations, made in the metropolis, and at various places around It, Vol. 1–3*London: Harvey and Darton. http://ci.nii.ac.jp/ncid/BB17291587.

Huang, G., Zhou, W., & Cadenasso, M. L. (2010). Understanding the relationship between urban land surface temperature, landscape heterogeneity and social structure. *International Geoscience and Remote Sensing Symposium*. https://ieeexplore.ieee.org/document/5649806.

Huang, G., Zhou, W., & Cadenasso, M. L. (2011). Is everyone hot in the city? Spatial pattern of land surface temperatures, land cover and neighborhood socioeconomic characteristics in Baltimore, MD. *Journal of Environmental Management, 92*(7), 1753–1759. https://doi.org/10.1016/j.jenvman.2011.02.006.

Imhoff, M. L., Zhang, P., Wolfe, R. E., & Bounoua, L. (2010). Remote sensing of the urban heat island effect across biomes in the continental USA. *Remote Sensing of Environment, 114*(3), 504–513. https://doi.org/10.1016/j.rse.2009.10.008 2010.

Kim, J. H., Gu, D., Sohn, W., Kil, S. H., Kim, H., & Lee, D. K. (2016). Neighborhood landscape spatial patterns and land surface temperature: An empirical study on single-family residential areas in Austin, Texas. *International Journal of Environmental Research and Public Health, 13*(9), 880. https://doaj.org/toc/1660-4601.

Kinney, P. L., O'Neill, M. S., Bell, M. L., & Schwartz, J. (2008). Approaches for estimating effects of climate change on heat-related deaths: Challenges and opportunities. *Environmental Science & Policy, 11*(1), 87–96. https://doi.org/10.1016/j.envsci.2007.08.001.

Kropf, K. (2009). Aspects of urban form. *Urban Morphology, 13*(2), 105–120. http://refhub.elsevier.com/S0264-2751(18)31518-X/rf0295.

Lesage, J. P., & Pace, R. K. (2014). The biggest myth in spatial econometrics. *Econometrics, 2*(4), 1–33. https://doi.org/10.2139/ssrn.1725503.

Li, X. X., & Norford, L. K. (2016). Evaluation of cool roof and vegetations in mitigating urban heat island in a tropical city, Singapore. *Urban Climate, 16*, 59–74. https://doi.org/10.1016/j.uclim.2015.12.002.

Li, J., Song, C., Cao, L., Zhu, F., Meng, X., & Wu, J. (2011). Impacts of landscape structure on surface urban heat islands: A case study of Shanghai, China. *Remote Sensing of Environment, 115*(12), 3249–3263. https://doi.org/10.1016/j.rse.2011.07.008.

Li, L., Tan, Y., Ying, S., Yu, Z., Li, Z., & Lan, H. (2014). Impact of land cover and population density on land surface temperature: Case study in Wuhan. *China. Journal of Applied Remote Sensing, 8*(1), 084993. https://doi.org/10.1117/1.JRS.8.084993.

Li, S., Zhao, Z., Miaomiao, X., & Wang, Y. (2010). Investigating spatial non-stationary and scale-dependent relationships between urban surface temperature and environmental factors using geographically weighted regression. *Environmental Modelling & Software, 25*(12), 1789–1800. http://www.sciencedirect.com/science/article/pii/S1364815210002008.

Li, X., Li, W., Middel, A., Harlan, S. L., Brazel, A. J., & Turner, B. (2016). Remote sensing of the surface urban heat island and land architecture in Phoenix, Arizona: Combined effects of land composition and configuration and cadastral-demographic-economic factors. *Remote Sensing of Environment, 174*, 233–243. https://doi.org/10.1016/j.rse.2015.12.022.

Li, Y., Zhang, H., & Kainz, W. (2012). Monitoring patterns of urban heat islands of the fast-growing Shanghai metropolis, China: Using time-series of Landsat TM/ETM + data. *International Journal of Applied Earth Observation and Geoinformation, 19*, 127–138. https://doi.org/10.1016/j.jag.2012.05.001.

Li, X., Zhou, W., Ouyang, Z., Xu, W., & Zheng, H. (2012). Spatial pattern of greenspace affects land surface temperature: evidence from the heavily urbanized Beijing metropolitan area, China. *Landscape Ecology, 27*(6), 887–898. https://doi.org/10.1007/s10980-012-9731-6.

Lo, C. P., Quattrochi, D. A., & Luvall, J. C. (1997). Application of high-resolution thermal infrared remote sensing and GIS to assess the urban heat island effect. *International Journal of Remote Sensing, 18*(2), 287–304. https://doi.org/10.1080/014311697219079.

Lynch, K. (1981). *A theory of good city form.* Cambridge, Mass: MIT Press. http://www.ijirset.com/upload/2016/january/109_25_THEORY.pdf.

Matthews, H. A. (1937). Reality in climate: The results of recent microclimatological studies with special reference to temperatures. *Geography, 22*, 87–100 McBoyle.

Matuschek, O., & Matzarakis, A. (2010). Estimation of sky view factor in complex environment as a tool for applied climatological studies. *Berichte des Meteorologischen Instituts der Albert-Ludwigs-Universität Freiburg, 20*, 534–539. http://refhub.elsevier.com/S2210-6707(17)31513-5/sbref0160.

Middel, A., Hab, K., Brazel, A. J., Martin, C. A., & Guhathakurta, S. (2014). Impact of urban form and design on mid-afternoon microclimate in Phoenix Local Climate Zones. *Landscape and Urban Planning, 122*, 16–28. https://doi.org/10.1016/j.landurbplan.2013.11.004.

Middel, A., Lukasczyk, J., & Maciejewski, R. (2017). Sky view factors from synthetic fish eye photos for thermal comfort routing—A case study in Phoenix, Arizona. *Urban Planning, 2*(1), 19–30. https://doi.org/10.17645/up.v2i1.855.

Mitchell, B., & Chakraborty, J. (2014). Urban heat and climate justice: A landscape of thermal inequity in Pinellas County, Florida. *Geographical Review, 104*(4), 459–480. https://doi.org/10.1111/j.1931-0846.2014.12039.x.

Moran, P. A. P. (1950). Notes on continuous stochastic phenomena. *Biometrika, 137*, 7–23. https://doi.org/10.1093/biomet/37.1-2.17.

Moyer, A. N., & Hawkins, T. W. (2017). River effects on the heat island of a small urban area. *Urban Climate, 21*, 262–277. https://doi.org/10.1016/j.uclim.2017.07.004.

Oke, T. R. (1979). *Review of urban climatology 1973–1976* (No. 04; QC875. 5, 04.)http://ci.nii.ac.jp/ncid/BA10866162.

Oke, T. R. (1987). Boundary layer climates. *Earth Science Reviews, 27*(3), 265. https://doi.org/10.4324/9780203407219.

Qin, Z. H., Li, W. J., Xu, B., Chen, Z. X., & Liu, J. (2004). Estimation of surface specific emissivity in terrestrial satellites in the TM6 band. *Remote Sensing of Land & Resources, 16*(3), 28–32 In Chinese.

Ren, Y., Deng, L. Y., Zuo, S. D., Song, X. D., & Li, Z. W. (2016). Quantifying the influences of various ecological factors on land surface temperature of urban forests. *Environmental Pollution, 216*(216), 519–529.

Rinner, C., & Hussain, M. (2011). Toronto's urban heat island—Exploring the relationship between land use and surface temperature. *Remote Sensing, 3*(6), 1251–1265. https://

doi.org/10.3390/rs3061251.
Sailor, D. J., & Lu, L. (2004). A top-down methodology for developing diurnal and seasonal anthropogenic heating profiles for urban areas. *Atmospheric Environment, 38*(17), 2737–2748. https://doi.org/10.1016/j.atmosenv.2004.01.034.
Schwarz, N., & Manceur, A. M. (2015). Analyzing the influence of urban forms on surface urban heat islands in Europe. *Journal of Urban Planning and Development-Asce, 141*(3), Article A4014003. https://doi.org/10.1061/(ASCE)UP.1943-5444.0000263.
Sharifi, A. (2019). Urban form resilience: A meso-scale analysis. *Cities, 93*, 238–252. https://doi.org/10.1016/j.cities.2019.05.010.
Shen, H., Huang, L., Zhang, L., Wu, P., & Zeng, C. (2016). Long-term and fine-scale satellite monitoring of the urban heat island effect by the fusion of multi-temporal and multi-sensor remote sensed data: A 26-year case study of the city of Wuhan in China. *Remote Sensing of Environment, 172*, 109–125. https://doi.org/10.1016/j.rse.2015.11.005.
Skoulika, F., Santamouris, M., Kolokotsa, D., & Boemi, N. (2014). On the thermal characteristics and the mitigation potential of a medium size urban park in Athens, Greece. *Landscape and Urban Planning, 123*, 73–86. https://doi.org/10.1016/j.landurbplan.2013.11.002.
Sobrino, J. A., Jiménez-Muñoz, J. C., & Paolini, L. (2004). Land surface temperature retrieval from Landsat TM 5. *Remote Sensing of Environment, 90*(4), 434–440. https://doi.org/10.1016/j.rse.2004.02.003.
Steeneveld, G. J., Koopmans, S., Heusinkveld, B. G., & Theeuwes, N. E. (2014). Refreshing the role of open water surfaces on mitigating the maximum urban heat island effect. *Landscape and Urban Planning, 121*(1), 92–96. https://doi.org/10.1016/j.landurbplan.2013.09.001.
Stewart, I. (2011). *Redefining the urban heat island.* Vancouver: The University of British Columbia. https://open.library.ubc.ca/media/stream/pdf/24/1.0072360/5.
Stewart, I. D., & Oke, T. R. (2012). Local climate zones for urban temperature studies. *Bulletin of the American Meteorological Society, 93*(12), 1879–1900. https://doi.org/10.1175/BAMS-D-11-00019.1.
Streutker, D. R. (2003). Satellite-measured growth of the urban heat island of Houston. *Texas. Remote Sensing of Environment, 85*(3), 282–289. https://doi.org/10.1016/S0034-4257(03)00007-5.
Sun, Q., Wu, Z., & Tan, J. (2012). The relationship between land surface temperature and land use/land cover in Guangzhou, China. *Environmental Earth Sciences, 65*(6), 1687–1694. https://rd.springer.com/content/pdf/10.1007%2Fs12665-011-1145-2.pdf.
Taleghani, M., Kleerekoper, L., Tenpierik, M., & Den Dobbelsteen, A. V. (2015). Outdoor thermal comfort within five different urban forms in the Netherlands. *Building and Environment, 83*, 65–78. https://doi.org/10.1016/j.buildenv.2014.03.014.
Tsai, Y.-H. (2005). Quantifying urban form: Compactness versus' Sprawl'. *Urban Studies, 42*(1), 141–161. https://doi.org/10.1080/0042098042000309748.
Unger, J. (2009). ). Connection between urban heat island and sky view factor approximated by a software tool on a 3D urban database. *International Journal of Environment and Pollution, 36*, 59–80. http://real.mtak.hu/id/eprint/5603.
Voogt, J. A., & Oke, T. R. (2003). Thermal remote sensing of urban climates. *Remote Sensing of Environment, 86*(3), 370–384. https://doi.org/10.1016/S0034-4257(03)00079-8.
Watson, I. D., & Johnson, G. T. (1987). Graphical estimation of sky view-factors in urban environments. *Journal of Climatology, 7*(2), 193–197. https://doi.org/10.1002/joc.3370070210.
Wei, R., Song, D., Wong, N. H., & Martin, M. (2016). Impact of urban morphology parameters on microclimate. *Procedia Engineering,* 142–149. https://doi.org/10.1016/j.proeng.2016.10.017.
Weng, Q. (2009). Thermal infrared remote sensing for urban climate and environmental studies: Methods, applications, and trends. *ISPRS Journal of Photogrammetry and Remote Sensing, 64*(4), 335–344. https://doi.org/10.1016/j.isprsjprs.2009.03.007.
Whitehand, J. W. R. (1992). Recent advances in urban morphology. *Urban Studies, 29*(3-4), 619–636. https://doi.org/10.1080/00420989220080591.
Xiao, R., Weng, Q., Ouyang, Z., Li, W., Schienke, E. W., & Zhang, Z. (2008). Land surface temperature variation and major factors in Beijing, China. *Photogrammetric Engineering and Remote Sensing, 74*(4), 451–461. https://doi.org/10.14358/PERS.74.4.451.
Yang, J., Su, J., Xia, J., Jin, C., & Ge, Q. (2018). The impact of spatial form of urban architecture on the urban thermal environment: A case study of the Zhongshan district, Dalian, China. *IEEE Journal of Selected Topics in Applied Earth Observations and Remote Sensing, 11*(10), 1–8. https://doi.org/10.1109/JSTARS.2018.2808469.
Yin, C., Yuan, M., Lu, Y., Huang, Y., & Liu, Y. (2018). Effects of urban form on the urban heat island effect based on spatial regression model. *The Science of the Total Environment,* 696–704. https://doi.org/10.1016/j.scitotenv.2018.03.350.
Yong, S. U., Wen, H. U., & Zhao, R. (2004). The ecological system design methods based on the dominant ecological gene in the urban hub: and the application in the urban hub of Shapingba, Chongqing. *Urban Planning Forum,* (05), 44–49 In Chinese.
Yuan, F., & Bauer, M. E. (2007). Comparison of impervious surface area and normalized difference vegetation index as indicators of surface urban heat island effects in Landsat imagery. *Remote Sensing of Environment, 106*(3), 375–386. https://doi.org/10.1016/j.rse.2006.09.003.
Yue, W., & Tan, W. (2007). The relationship between land surface temperature and NDVI with remote sensing: Application to Shanghai Landsat 7 ETM+ data. *Journal of remote sensing, 28*(15), 3205–3226. https://doi.org/10.1080/01431160500306906.
Zhang, W., Zheng, C., & Chen, F. (2019). Mapping heat-related health risks of elderly citizens in mountainous area: A case study of Chongqing, China. *The Science of the Total Environment, 663*, 852–866.
Zhao, C., Fu, G., Liu, X., & Fu, F. (2011). Urban planning indicators, morphology and climate indicators: A case study for a north-south transect of Beijing, China. *Building and Environment, 46*(5), 1174–1183. https://doi.org/10.1016/j.buildenv.2010.12.009.
Zhou, W., Huang, G., & Cadenasso, M. L. (2011). Does spatial configuration matter? Understanding the effects of land cover pattern on land surface temperature in urban landscapes. *Landscape and Urban Planning, 102*(1), 54–63. https://doi.org/10.1016/j.landurbplan.2011.03.009.